Mon. Not. R. Astron. Soc. **385,** 1076–1086 (2008) doi:10.1111/j.1365-2966.2008.12915.x

Infrared spectroscopic study of a selection of AGB and post-AGB stars

V. Venkata Raman⋆ and B. G. Anandarao⋆
Physical Research Laboratory (PRL), Navrangpura, Ahmedabad 380009, India

Accepted 2008 January 3. Received 2007 December 3; in original form 2007 June 27

ABSTRACT

We present here near-infrared spectroscopy in the *H* and *K* bands of a selection of nearly 80 stars that belong to various asymptotic giant branch (AGB) types, namely S type, M type and SR type. This sample also includes 16 post-AGB (PAGB) stars. From these spectra, we seek correlations between the equivalent widths of some important spectral signatures and the infrared colours that are indicative of mass-loss. Repeated spectroscopic observations were made on some PAGB stars to look for spectral variations. We also analyse archival *Spitzer* mid-infrared spectra on a few PAGB stars to identify spectral features due to polycyclic aromatic hydrocarbon (PAH) molecules providing confirmation of the advanced stage of their evolution. Further, we model the spectral energy distributions (SEDs) of the stars (compiled from archival data) and compare circumstellar dust parameters and mass-loss rates in different types.

Our near-infrared spectra show that in the case of M- and S type stars, the equivalent widths of the CO(3–0) band are moderately correlated with infrared colours, suggesting a possible relationship with mass-loss processes. A few PAGB stars revealed short-term variability in their spectra, indicating episodic mass-loss: the cooler stars showed in CO first overtone bands and the hotter ones showed in H I Brackett lines. Our spectra on IRAS 19399+2312 suggest that it is a transition object. From the *Spitzer* spectra, there seems to be a dependence between the spectral type of the PAGB stars and the strength of the PAH features. Modelling of SEDs showed among the M and PAGB stars that the higher the mass-loss rates, the higher the [$K - 12$] colour in our sample.

Key words: techniques: spectroscopic – stars: AGB and post-AGB – circumstellar matter – stars: evolution – stars: mass-loss – dust, extinction.

1 INTRODUCTION

During their asymptotic giant branch (AGB) stage, intermediate-mass stars undergo substantial mass-loss triggered by pulsation shocks and radiation pressure (e.g. Willson 2000; van Winckel 2003). Near-infrared (near-IR) spectroscopy is one of the recognized tools to study the mass-loss process (e.g. Kleinmann & Hall 1986; Volk, Kwok & Hrivnak 1999; Lancon & Wood 2000; Bieging, Rieke & Rieke 2002; Winters et al. 2003). The near-IR *JHK* bands, contain several important diagnostic lines that can be used as signatures to probe the atmospheres of these stars (Hinkle, Hall & Ridgway 1982).

One of the most dramatic manifestations of the AGB stage is the high rate of mass-loss that is mainly attributed to pulsational levitation of atmosphere followed by expulsion of matter by the radiation pressure (Wood 1979; Bowen 1988; Gail & Sedlmayr 1988; Vassiliadis & Wood 1993; Habing 1996; Feast 2000; Willson 2000; Winters et al. 2000; Woitke 2003; Garcia-Lario 2006). One of the issues that we would address is the possible signatures of pulsational mass-loss in the spectra of AGB stars. We would also like to study the IR spectral signatures that the intermediate-mass stars leave while evolving beyond AGB stage to become planetary nebulae (PNe) (e.g. Kwok 2000).

In this work we report near-IR (*H* and *K* bands) spectroscopy on a selection of about 80 AGB stars of different types, namely M type, S type, semiregular variables (SR) and post-AGB (PAGB) candidates (Section 2). In Section 3.1, we try to seek significant differences among these types and correlate spectral signature strengths with pulsation parameters or mass-loss indicators (such as the IR colour indices) in case of M, S and SR types.

Further, we present the *Spitzer* archival spectra in the mid-IR region on a few PAGB stars in order to find out the evolutionary stage of these stars in terms of the spectral features seen in the spectra (Section 3.2). Following this, using the DUSTY code, we model the IR spectral energy distributions (SEDs) of these sample stars, constructed from archival data in the visible, near- and far-IR regions to investigate basic differences in the photospheric and circumstellar parameters among the various types of AGB stars (Section 3.3). Some interesting aspects on variation of spectral lines in a few PAGB

⋆E-mail: vvenkat@prl.res.in (VVR); anand@prl.res.in (BGA)

© 2008 The Authors. Journal compilation © 2008 RAS

stars are discussed in Section 4. Section 5 lists important conclusions of the present work.

2 NEAR-INFRARED SPECTROSCOPIC OBSERVATIONS

Near-IR spectroscopic observations were made in the *J* (only for some of the sample PAGB stars), *H* and *K* bands on the selection of stars, using the NICMOS-3 near-IR camera/spectrograph at the Cassegrain focus of the 1.2-m telescope at Mt Abu, Western India, during the period 2003-07. The observations were made at a spectral resolution of ∼1000. Spectrophotometric standard stars of A0V type were used for each programme star at similar air mass to remove the telluric absorptions and for relative flux calibration (cf. Lancon & Rocca-Volmerange 1992). For sky background subtraction, two traces were taken for each star for each cycle of integration at two spatially separated positions along the slit within 30 arcsec. Typical overall integration times varied between 0.6 and 160 s for the brightest and faintest stars in our sample (in each of the three bands). The atmospheric OH vibration–rotation lines were used to calibrate wavelength. The H I absorption lines from the standard star spectra are removed by interpolation. The resulting spectra of the standard star were used for the removal of telluric lines from the programme star by ratioing. The ratioed spectra were then multiplied by a blackbody spectrum at the effective temperature corresponding to the standard star to obtain the final spectra. Typically the signal-to-noise ratios (S/N values) at the strongest and the weakest spectral features varied between 100 and 3, respectively. Data processing was done using standard spectroscopic tasks (e.g. APALL) inside IRAF.

2.1 The sample stars

The programme stars were selected from published literature/catalogues (Fouquet et al. 1992; Kerschbaum & Hron 1994; Chen, Gao & Jorissen 1995; Wang & Chen 2002; Stasinska et al. 2006). Our sample contains about 80 stars with the selection based on the observability at Mt Abu during the period November–May and *JHK*-band magnitudes brighter than 8–9. Among these stars, 30 are M type; 17 S type; 15 SR type and 16 are PAGB stars [some of which are known to be transition/proto-PNe (PPNe), see Ueta et al. 2003 and Kelly & Hrivnak 2005]. The greater bias towards M types in the sample is due to the fact that they are brighter in *K* band than the others. Tables 1–4 list all the stars in the four categories along with the $[H-K]$ and $[K-12]$ colours computed from Two Micron All Sky Survey (2MASS) and IRAS photometric archival data. The phases (ϕ) of the variable stars of M and SR types, corresponding to the dates of our observations, are also listed in the tables (epochs taken from Kholopov et al. 1988). The spectral types are taken from SIMBAD data base.

3 RESULTS AND DISCUSSION

Fig. 1 shows some typical spectra for different types considered here. In general, we find in the AGB stars, the photospheric absorption lines of Na I doublet at 2.21 μm, Ca I triplet at ∼2.26 μm, as well as Mg I at 1.708 μm in all the sample stars. Brackett

Table 1. 2MASS and IRAS colours and Mt Abu EWs (in Å) of the spectral features of the sample M stars.

Star	Spectral type	ϕ	$H-K$	$K-12$	CO(3–0)	CO(4–1)	CO(*H*)	CO(2–0)	CO(3–1)	CO(*K*)	$\dot{M}$
02234−0024	M4e	0.34	0.44	2.31	16.1	7.8	51.5	21.1	6.9	61.9	2.6(−6)†
03082+1436	M5.5e	0.33	0.45	1.99	11.3	9.2	64.2	25.1	13.3	62.3	9.8(−7)†
03489−0131	M4III	–	0.31	1.86	4.8	5.3	61.9	18.4	20.2	45.9	1.3(−6)
04352+6602	Sev	0.44	0.50	1.22	–	–	–	31.8	29.8	101.2	1.4(−7)†
05265−0443	M7e	0.57	0.49	1.32	13.6	10.1	53.1	15.1	7.8	22.9	4.6(−7)†
05495+1547	S7.5	0.49	0.59	2.79	11.6	8.4	47.4	11.9	16.0	47.6	3.5(−6)
06468−1342	S	–	0.52	1.03	14.5	16.6	85.0	32.9	31.2	110.6	–
06571+5524	Se	0.59	0.64	1.67	20.0	22.1	105.6	18.3	25.6	52.8	1.7(−6)†
07043+2246	S6.9e	0.36	0.18	1.17	11.6	13.9	77.0	34.3	28.8	98.8	3.1(−7)†
07092+0735	Se	0.30	0.71	3.02	16.4	15.4	72.1	20.5	25.8	81.0	2.9(−6)
07197−1451	S	0.26	0.55	2.32	11.8	8.0	65.0	22.3	9.7	43.5	4.6(−6)
07299+0825	M7e	0.57	0.36	1.90	16.2	10.5	64.1	26.8	14.1	65.3	8.5(−7)†
07462+2351	SeV	0.96	0.52	-0.90	12.3	13.8	68.8	28.1	33.9	108.0	–
07537+3118		0.09	0.53	1.40	13.7	9.9	76.5	22.8	25.0	77.5	–
07584−2051	S2,4e	0.19	0.44	1.00	12.6	11.0	78.4	21.2	17.9	39.1	–
08188+1726	SeV	–	0.41	2.28	14.3	13.6	66.1	22.2	24.8	71.3	–
08308−1748	S	–	0.43	0.72	10.1	15.9	72.6	25.7	19.1	92.9	1.7(−7)
08416−3220		–	0.41	0.97	12.2	14.2	75.8	33.0	35.0	105.3	–
08430−2548		–	0.46	1.51	12.2	13.0	68.3	19.6	16.6	80.2	–
09411−1820	Me	0.31	0.49	1.63	5.1	7.3	33.2	8.5	5.7	22.1	7.9(−7)†
12372−2623	M4	0.92	0.40	1.39	9.9	14.8	64.2	20.2	23.8	50.8	–
17001−3651	M	0.70	0.58	2.17	9.6	8.9	57.0	11.3	8.9	35.8	1.9(−6)†
17186−2914	S	–	0.70	1.76	14.5	13.2	80.7	23.9	26.1	89.2	2.9(−6)
17490−3502	M	0.60	0.54	2.26	16.4	16.1	78.1	24.6	17.6	95.8	–
17521−2907	Se	0.11	0.56	1.64	18.9	19.5	88.4	20.1	21.9	71.8	4.6(−6)
18508−1415	SeV	0.44	0.38	1.00	3.4	5.1	64.3	8.8	5.5	31.1	–
19111+2555	S	0.57	0.80	4.36	19.1	17.6	66.8	13.3	11.2	24.5	4.6(−6)†
19126−0708	S...	0.90	0.79	3.81	21.6	19.1	102.0	21.5	23.5	59.4	2.9(−6)†
19354+5005	S...	0.24	0.52	2.28	26.6	22.8	108.0	30.2	33.8	98.2	1.5(−6)†
23041+1016	M7e	0.87	0.52	2.40	7.3	9.0	50.7	12.4	6.3	18.7	1.5(−6)†

© 2008 The Authors. Journal compilation © 2008 RAS, MNRAS **385,** 1076–1086

Table 2. 2MASS and IRAS colours and Mt Abu EWs (in Å) of spectral features of the sample S stars.

Star	Spectral type	$H-K$	$K-12$	CO(3–0)	CO(4–1)	CO(H)	CO(2–0)	CO(3–1)	CO(K)	$\dot{M}$
04599+1514	M0	0.49	0.96	12.8	17.3	80.8	24.2	28.6	99.4	1.4(−7)†
05036+1222		0.60	1.09	12.7	15.1	80.9	26.2	28.1	54.3	–
05374+3153	M2Iab	0.16	1.44	13.7	12.2	77.5	21.6	26.6	88.3	7.3(−7)†
07247−1137	Sv...	0.34	0.85	8.6	10.7	57.8	25.8	19.1	74.5	–
07392+1419	M3II–III	0.09	−1.44	5.3	8.4	38.9	16.7	14.7	55.3	7.3(−7)
09070−2847	S	0.25	0.91	10.7	12.8	74.1	22.1	37.1	59.2	–
09152−3023		0.47	1.21	4.0	9.4	44.2	18.1	14.4	39.1	–
10538−1033	M...	0.29	0.74	8.1	4.5	44.6	22.9	9.6	64.9	–
11046+6838	M...	0.40	0.39	3.7	9.5	41.1	15.0	10.4	54.7	–
12219−2802	S	0.30	0.72	9.2	9.4	57.0	22.1	17.8	69.8	–
12417+6121	SeV	0.41	0.95	16.7	18.0	82.4	28.2	29.5	92.2	1.0(−7)†
13421−0316	K5	0.22	0.57	–	8.3	40.9	20.0	14.9	59.8	–
13494−0313	M...	0.42	0.56	3.0	9.2	55.5	17.4	20.0	47.4	–
14251−0251	S...	0.34	0.71	3.7	9.1	45.8	20.2	16.7	60.0	–
15494−2312	S	0.38	0.62	5.1	8.1	46.1	19.8	17.2	59.3	–
16205+5659	M...	0.18	0.78	5.4	7.1	45.3	13.0	19.1	61.6	–
16209−2808	S	0.54	0.92	10.7	13.6	73.9	21.9	27.2	79.5	1.0(−7)

Table 3. 2MASS and IRAS colours and Mt Abu EWs (in Å) of spectral features of the sample SR stars.

Star	Spectral type	ϕ	$H-K$	$K-12$	CO(3–0)	CO(4–1)	CO(H)	CO(2–0)	CO(3–1)	CO(K)	$\dot{M}$
04030+2435	S4.2V	–	0.40	0.63	4.1	8.3	45.0	16.2	17.9	34.1	–
04483+2826	CII	–	0.38	1.04	7.0	10.9	60.3	24.5	17.6	58.3	1.4(−7)
05213+0615	M4	0.41	0.39	1.37	9.3	11.1	64.8	19.3	21.4	56.9	–
05440+1753	S0.V	0.33	0.66	1.89	22.7	19.5	99.5	33.2	30.3	88.1	1.4(−6)
06333−0520	M6	0.85	0.38	1.20	19.7	10.1	77.8	19.1	24.8	61.5	1.7(−7)
08272−0609	M6e	–	0.40	1.47	11.3	7.8	51.7	19.1	15.1	81.4	5.6(−7)
08372−0924	M5II	–	0.36	1.57	5.5	6.5	52.3	18.5	12.4	49.0	1.7(−7)
08555+1102	M5III	–	0.26	1.28	7.4	7.9	61.8	15.5	13.9	43.7	2.4(−7)
09076+3110	M6IIIaSe	–	0.31	1.20	13.5	11.6	65.9	18.5	18.8	56.7	3.8(−7)†
10436−3459	S	–	0.37	1.61	10.5	15.4	61.2	30.3	23.9	79.0	9.5(−7)†
15492+4837	M6S	0.77	0.40	1.58	12.7	13.0	63.8	19.9	24.5	44.4	9.5(−7)†
16334−3107	S4.7:.V	–	0.43	1.13	15.0	22.9	93.4	22.5	29.7	104.8	1.0(−7)†
17206−2826	M...	–	0.42	0.82	10.3	11.4	68.1	15.2	19.6	63.8	1.0(−7)†
17390+0645	SV...	–	0.36	0.92	12.1	7.6	56.7	29.8	14.2	70.9	–
19497+4327		–	0.60	0.82	6.7	11.5	59.2	25.2	18.1	73.8	–

Table 4. 2MASS and IRAS colours and Mt Abu EWs (in Å) of spectral features of the sample PAGB stars.

Star	Spectral type	$H-K$	$K-12$	Paβ	Brγ	CO(K)	21 μm	T_d	$\dot{M}$
Z02229+6208	G9a	0.44	6.38	–	9.2	8.4	–	300	2.9(−5)
04296+3429	G0Ia	0.49	7.34	–	4.1	17.7	−2.11	270	4.5(−5)†
05113+1347	G8Ia	0.25	5.98	–	6.5	12.9	–	350	2.1(−5)
06556+1623	Bpe	1.11	5.10	–	−52.4	–	–	1200/150	1.0(−5)
07134+1005	F5Ia	0.10	6.45	–	5.1	–	−1.73	280	2.3(−5)†
07284−0940	K0Ibpv	0.23	5.64	–	–	10.9	–	450	1.0(−5)
07430+1115	G5Ia	0.44	6.35	–	3.9	28.9	–	320	3.3(−5)
17423−1755	Be	1.48	5.30	–	−5.6	−23.6	–	125	4.9(−6)†
18237−0715	Be	0.55	2.29	−25.6	−14.9	–	–	70	5.8(−6)
19114+0002	G5Ia	0.27	4.84	–	5.4	–	–	120	4.9(−5)†
19157−0247	B1III	1.19	5.76	–	–	−10.8	–	270	1.1(−6)†
19399+2312	B1e	0.11	4.80	−6.2	−15.6	–	–	–	–
22223+4327	F9Ia	0.24	4.44	7.5	5.8	–	−1.31	125	1.0(−5)†
22272+5435	G5Ia	0.38	5.55	4.4	3.4	30.2	−0.83	250	1.6(−5)†
22327−1731	A0III	0.90	4.95	3.8	–	28.7	–	800	5.0(−6)
23304+6147	G2Ia	0.36	6.48	3.4	5.1	12.8	−2.53	250	3.5(−5)†

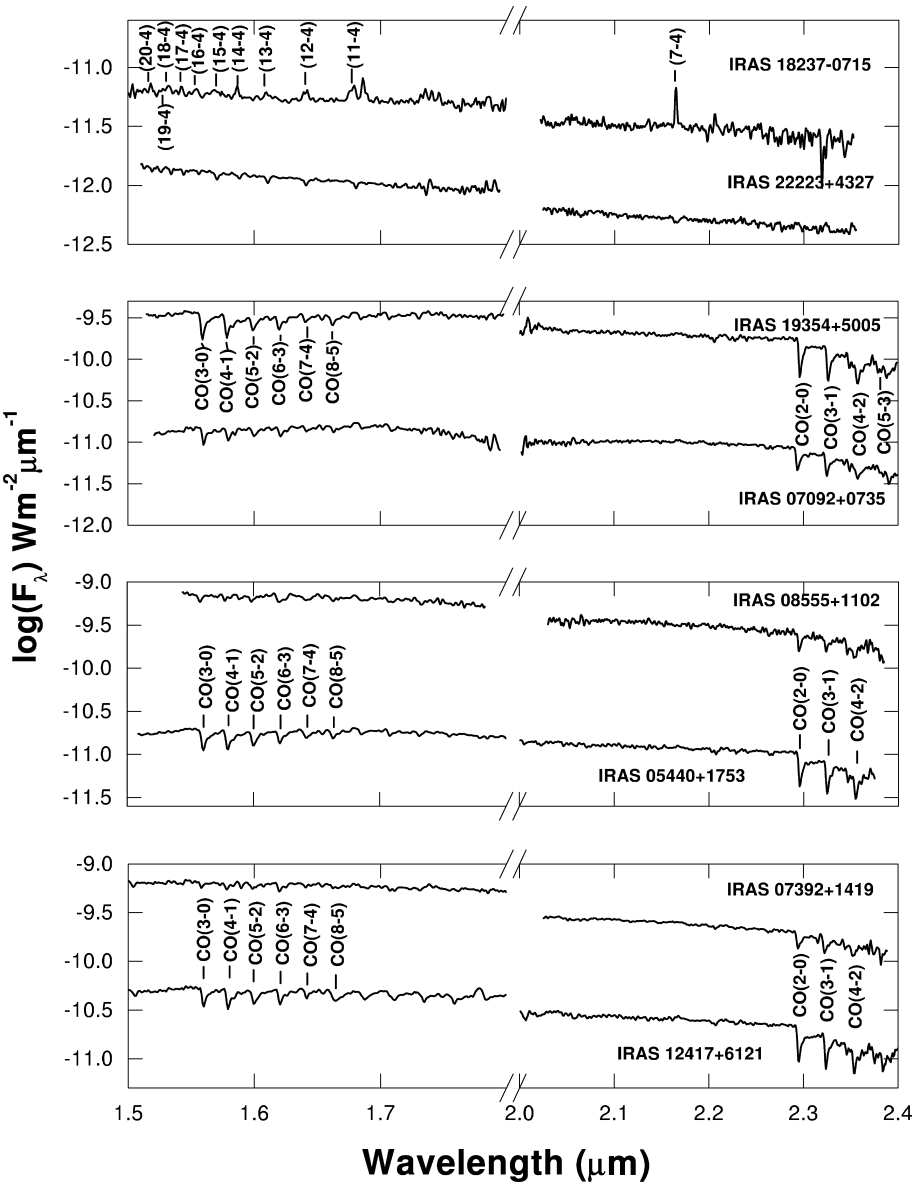

Figure 1. Mt Abu near-IR spectra of a selection of AGB and PAGB stars. From top to bottom the panels show PAGB, M, SR and S type stars giving two examples per category.

series lines of H I were found mostly among the PAGB stars where a hotter central source is believed to be present. In addition, the CO vibration–rotation lines of first and second overtone bands ($\Delta v = 2$ and 3, respectively) were seen in a large number of M, S and SR type stars and in a few PAGB stars. Some PAGB stars showed H I Brackett emission lines (IRAS 06556+1623, 17423−1755, 18237−0715 and 19399+2312 for the last one of which our spectra are new) and an indication of fainter emission in CO. This could be due to the fact that as the central star becomes hot, the CO lines become progressively weaker and finally disappear when CO dissociates (at 11.2 eV). Around this time the H I recombination lines start becoming prominent in emission. Our spectra on IRAS 06556+1623 and 17423−1755 are quite comparable to those of Garcia-Hernandez et al. (2002), with a faint detection of H_2 S(1) 1–0 line at 2.12 μm. For the PAGB object IRAS 22327−1731, our spectra showed for the first time absorption in H I lines and CO bands. Some of the PAGB objects that showed variability are discussed in Section 4. Equivalent widths (EWs) were computed for all the spectral features that are detected in our sample stars. The errors in the EWs are mainly from the S/N of the lines. To that extent the errors are estimated to be about 3 Å, mostly applicable to the low-S/N (∼3) line detections, such as the metallic lines; but for high-S/N ($\geqslant$5) line/bands the errors are $\leqslant$1 Å. Tables 1–4 list the EWs (in Å, positive for absorption and negative for emission) of the CO(3–0, 4–1) second overtone bands in *H* band, CO(2–0, 3–1) first overtone bands in *K* band and H I Brackett series lines (only for PAGB stars), for the programme stars of each category.

3.1 Correlations and their implications

Based on physical processes, very interesting correlations were found among spectral features observed in AGB stars (Kleinmann & Hall 1986; Lancon & Wood 2000; Bieging et al. 2002). We tried to see if our sample too shows these. Kleinmann & Hall (1986) and

© 2008 The Authors. Journal compilation © 2008 RAS, MNRAS **385,** 1076–1086

Bieging et al. (2002) have found that the CO(2–0) and CO(3–1) band head strengths are correlated. From the Tables 1–3, we can see this trend; in addition, one can see a correlation between CO(3–0) and CO(4–1) bands as well.

The first overtone bands of CO ($\Delta v = 2$) in the K band arise at $T \sim 800$ K partly in the photosphere and partly in the circumstellar envelopes; while the second overtone bands ($\Delta v = 3$) in the H band arise at $T \sim 3000$–4000 K entirely in the photospheric layers (e.g. Hinkle et al. 1982; Emerson 1996). As a result, the pulsational effects may be more pronounced in the $\Delta v = 3$ bands than in the $\Delta v = 2$ bands; while the former will reflect the circumstellar matter properties better. Thus we would expect a better correlation between EW of $\Delta v = 3$ bands with pulsation period P than the $\Delta v = 2$ bands. It should be noted here that for the CO bands the S/N is high (in many cases $\geqslant$5) and hence the errors in EW are $\leqslant$1 Å. Fig. 2 shows EWs of CO(3–0) and CO(2–0) plotted against the colour $[H - K]$ for M type stars. The phases of these variable stars are not necessarily the same between our observations and 2MASS or IRAS data acquisition (see Table 1 for phases during our observations). Also shown in Fig. 2 are the EWs of the CO lines from the S type stars (against the colour $[K - 12]$). The trend of correlation for CO(3–0) band is quite clear. For SR stars, we did not find any such trend.

In order to quantify the degree of correlation between two parameters, we have used the Spearman rank correlation method that does not assume any functional relationship between them (e.g. used by Loidl, Lancon & Jorgensen 2001). Fig. 2 shows only those correlations with CO(3–0) for which the rank coefficient (ρ) $\geqslant 0.50$ and its significance (s) $\leqslant 0.01$ (i.e. a chance occurrence of 1 in 100). We find that for M stars, for the CO(3–0) versus $[H - K]$, ρ is 0.50 with s of 0.008 (a chance occurrence of 8 in 1000); while for S stars, for CO(3–0) versus $[K - 12]$ ρ is 0.74 with s of 0.003. These are moderately significant correlations as may also be visually seen from the plots. In comparison, the coefficients and their significance are quite poor for the CO(2–0) plots in Fig. 2. For M stars, one can also see a trend in the CO ($\Delta v = 3$) versus log P better than CO($\Delta v = 2$) versus log P (not shown). Usually the mass-loss is correlated well with the pulsation period; as also by the colour indices $[H - K]$ and $[K - 12]$ (Whitelock et al. 1994). While the trends in Fig. 2 are certainly beyond the errors in EW, we find that the scatter is rather significant in the correlation plot between the CO(3–0) band EWs and $[H - K]$ and other mass-loss indicators (not shown) such as log P and $[K - 12]$, although it is much less in comparison to the plots for CO(2–0) band (only $[H - K]$ is shown). Lancon & Wood (2000) and Loidl et al. (2001) argued that in the case of carbon-rich AGB stars, the CO lines arise deeper in side the atmospheres (close to the photospheres) and hence may not respond to dynamical effects such as pulsations as much as those lines that arise in the outer atmospheres. In our sample M stars, a large number of them are oxygen-rich and hence the pulsational phase effects may be significant and can possibly account for the scatter in our plots.

3.2 *Spitzer* spectra on a few post-AGB objects – PAH and 21 μm features

We have searched the *Spitzer* archival spectroscopic data in the mid-IR region of 6–30 μm and succeeded in obtaining seven PAGB stars for which the data were available and unpublished and are not in the list of sources presented originally by Hrivnak, Volk & Kwok (2000). The raw spectra (post-basic calibrated data) were analysed using the *Spitzer* IRS Custom Extraction (SPICE) task under *Spitzer* data processing software packages. Interesting spectra in the wavelength range of 10–18 μm from these objects are shown in Fig. 3 (where in addition to the seven *Spitzer* stars, we have shown one more PAGB star, namely IRAS 22272+5435, reanalysed from the *ISO*

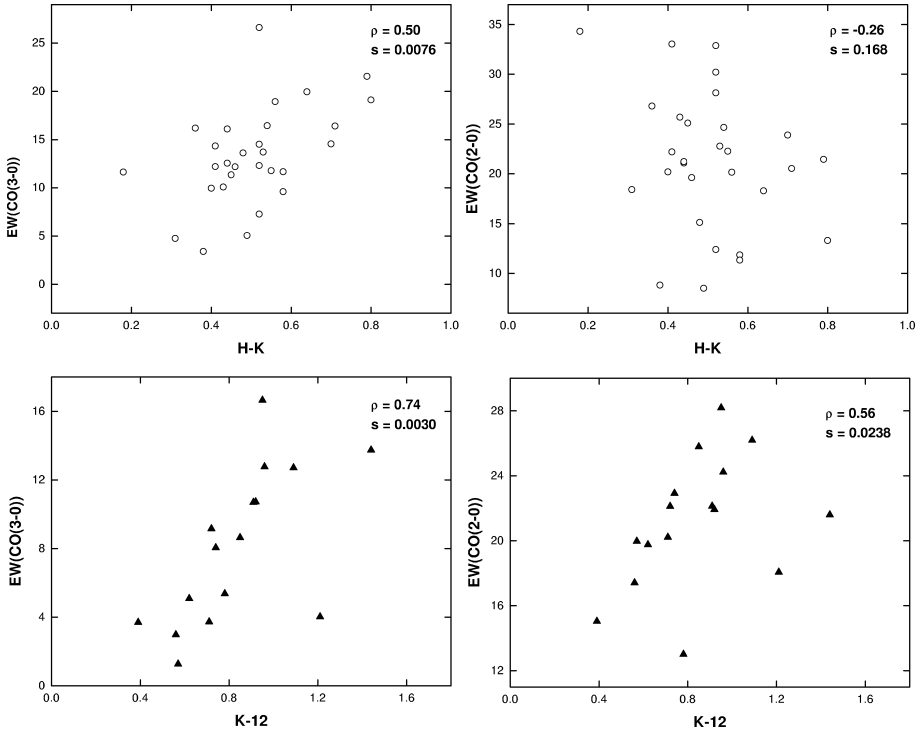

Figure 2. Plots of EWs (in Å) of the CO(3–0) line (left-hand panels) and CO(2–0) line (right-hand panels) with the IR colours $[H - K]$ for M stars (shown as open circles in top panels) and $[K - 12]$ for S type stars (filled triangles in bottom panels). The Spearman rank correlation coefficient (ρ) and its significance (s) are given in the corresponding figures.

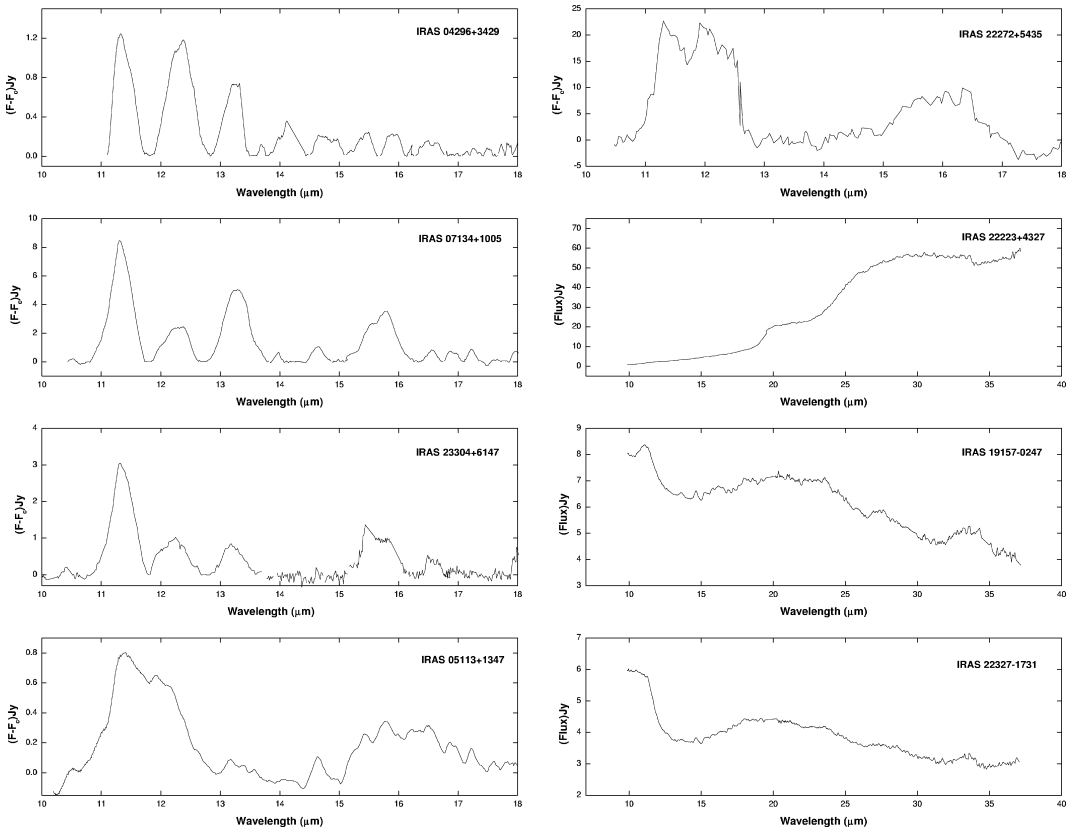

Figure 3. *Spitzer* spectra for some PAGB stars showing mid-IR PAH features in emission (for all the four spectra shown in the left-hand side panels and the one in the top right-hand panel, continuum was subtracted using (fifth-order) polynomial fitting in segments). The spectra for IRAS 22272+5435 were obtained by reanalysing the *ISO* data and shown here for comparison.

spectral archives). Of these eight stars, IRAS 19157−0247 and IRAS 22327−1731 are of early spectral types and showed nearly featureless continua (see Fig. 3). For the spectra of those stars that showed the in-plane and out-of-plane bending modes of C–H bonds in polycyclic aromatic hydrocarbon (PAH) molecules (e.g. Kwok 2004 and Tielens 2005), we have subtracted the continuum by (fifth-order) polynomial fitting in segments, in order to bring out the comparative strengths of the features. Fig. 4 shows the 6–10 μm spectra on two stars for which the data are available; these stars show the C–C stretching modes of 6.2 and 6.9 μm and the blended features around 8 μm due to C–C stretching and C–H in-plane bending modes. A comparison of the spectra in the region of 10–18 μm common to about six PAGB objects suggests that the intensity of the spectral features due to PAH molecules depends on the spectral type of the star – being weakest or shallowest for cooler stars than for relatively hotter stars. This can possibly be due to the ultraviolet (UV) radiation flux and the hardness that is available to excite the molecules (Tielens 2005).

We have computed the ratio of the EWs of the $F_{7.9}/F_{11.3}$ feature which is known to indicate whether the molecule is neutral or ionized (see Tielens 2005). We find that the PAGB star IRAS 04296+3429, having a ratio of 11.3, probably shows indications for ionized PAH molecules, while in IRAS 22272+5435, with a ratio of 0.8, neutrals may be predominant (see Figs 3 and 4). Further, the relative structure of PAHs may be inferred from the ratio of $F_{11.3}/F_{12.7}$: a large ratio indicates large compact PAHs, while a small ratio results when these molecules break up into smaller irregular structures (Hony et al. 2001; Peeters et al. 2002; Sloan et al. 2005; Tielens 2005). In our sample PAGB stars, we find (see Fig. 3) that the objects IRAS 07134+1005 and 23304+5147 have ratios of 4.7 and 3.6, respectively, and hence may have large compact PAH molecules compared to IRAS 04296+3429 that has a ratio of 0.8. In IRAS 05113+1347 and 22272+5435 the *Spitzer* spectra show wide features at 7–8 and 11–12 μm regions. Such broad features are usually attributed to more complex structures in PAH molecules (see Kwok 2004).

Since the PAH modes arise by absorption of UV photons, their presence indicates the onset of substantial UV flux from the central star and hence the onset of transition/PPN phase. Mt Abu spectra taken on all these objects do not show the H I Brackett series in emission; they are seen in absorption. Thus it is possible that the UV radiation is soft ($\leqslant$13.6 eV) as H ionization has not yet started in these objects.

Only three of our sample PAGB stars have *Spitzer* archival data beyond 18 μm, and all showed the 21-μm feature (Kwok, Volk & Hrivnak 1989, 1999; Volk, Kwok & Hrivnak 1999; Decin et al. 1998), which was attributed to TiC (von Helden et al. 2000) or SiC (Speck & Hofmeister 2004). Since these objects are already known to have the 21-μm feature (Volk et al. 1999), in Table 4 we give only the EWs of the feature (in μm), along with the EW for IRAS 07134+1005 computed from *ISO* archival data. All the properties of the observed feature (the peak wavelength, width and red-side asymmetry) resemble the SiC feature as shown by Speck & Hofmeister (2004).

© 2008 The Authors. Journal compilation © 2008 RAS, MNRAS **385,** 1076–1086

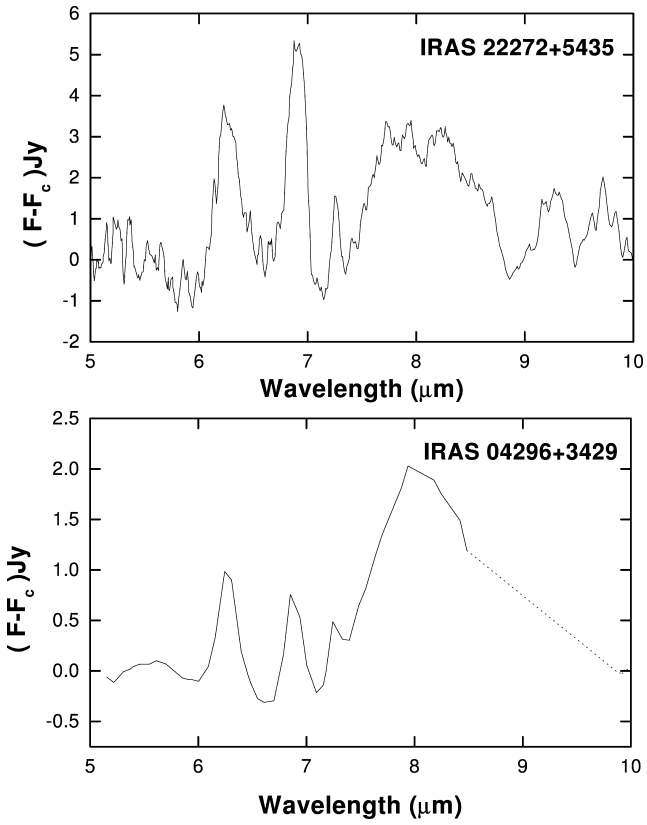

Figure 4. *Spitzer* spectra of IRAS 04296+3429 showing mid-IR (in the range 6–10 μm) PAH features in emission (continuum-subtracted as in Fig. 3). The spectra for IRAS 22272+5435 were obtained by reanalysing the *ISO* data and is shown here for comparison.

3.3 Modelling of infrared spectral energy distribution

Using the DUSTY code (Ivezic & Elitzur 1997), we have modelled the SEDs in the spectral region of 0.5–100 μm. This code incorporates full dynamical calculation for radiatively driven winds in AGB stars. The photometric data on all the programme objects were compiled mainly from 2MASS and IRAS archives. We have modelled the SEDs of all the programme stars except those that have upper limits (quality = 1) in IRAS data in more than one band. For a majority of the programme stars IRAS LRS data are not available. Even in the *ISO* archives we could get only a few stars. Therefore, we have modelled only the photometric fluxes, assuming silicate dust for M, S and SR types; while for most of the PAGB stars, we required carbonaceous dust. The dust grain data were taken from in-built tables in DUSTY. In a few cases we obtained data from DENIS and MSX archives as well. In the model that assumes spherical geometry, we fix stellar parameters like the photometric temperature (based on the visible and the near-IR data), inner dust shell temperature, type of dust and size distribution (MRN assumed) and opacity at 0.5 μm (usually taken value between 0.1 and 1.0). We have used density distribution relevant for modelling the radiatively driven winds in AGB stars as incorporated in to DUSTY by its authors. There would be 10–20 per cent uncertainties in all the model output parameters. We have generated nearly 150 models using several combinations of the above parameters. We then take the fluxes computed by the code and normalize with the observed 2-μm flux from each object and construct the model SEDs. A χ^2 test is performed to select the best fit model. In general the model shows that the M types have lower effective temperatures than the S and SR types. M types show higher opacities by a factor of 2, than the S and SR types; S type being lowest. However, the inner dust shell temperature for all the types were found to be in the range 450–700 K. The SEDs of PAGB stars showed, in general, double-humped but flatter trend than their AGB counterparts, indicating detached circumstellar shells (see e.g. Hrivnak & Kwok 1999). Since some of these are transition objects their spectral classes are much earlier than M types. The inner dust shell temperatures for most of the PAGB stars, as listed in Table 4, are found to be in the range of ∼100–300 K, significantly cooler than the values for AGB stars. A warmer dust shell was required in addition to the cooler one in one of the PAGB stars (1200 K for IRAS 06556+1623). The dust parameters that we obtained are in good agreement with those in the published literature. A few examples of SEDs of M, S, SR and PAGB stars and their model fits are shown in Figs 5–7, respectively. The DUSTY AGB star model estimates mass-loss rate also but with larger uncertainty of 30 per cent. The mass-loss rates (in $M_\odot$ yr^{-1}) thus obtained are listed in Tables 1–4 for all the types; the sign † shows stars for which the rates are independently available from CO rotational line observations by several authors, namely Loup et al. (1993), Sahai & Liechti (1995), Groenewegen & de Jong (1998), Jorissen & Knapp (1998), Winters et al. (2000) and Ramstedt et al. (2006) for M, S and SR stars; and Woodsworth, Kwok & Chen (1990), Likkel et al. (1991), Omont et al. (1993), Hrivnak & Kwok (1999), Bujarrabal et al. (2001), Hoogzaad et al. (2002) and Hrivnak & Bieging (2005) for PAGB stars. Our model mass-loss rates are in reasonably good agreement with those determined from CO rotational lines, for all cases. From Tables 1 and 4, one can see a clear trend of increase of mass-loss rate with increase of the colour $[K - 12]$ (e.g. Bieging et al. 2002). Basically most of our sample M type stars are in the ascending phase of their AGB stage and hence the mass-loss rate increases with the $[K - 12]$ index (see Whitelock et al. 1994 and Habing 1996); while the PAGB stars in our sample are already in the PPN stage, having just passed the superwind mass-loss event. Following this phase the mass-loss would decrease. In fact one can see (Table 4) that the mass-loss rates for hot PAGB stars are distinctly less than those for cooler ones, possibly indicating the decrease of mass-loss after a superwind event.

4 SPECTRAL VARIATIONS IN SOME PAGB OBJECTS

Most of the PAGB stars in our sample are identified as PPNe (see Ueta et al. 2003 and references therein). Repeated spectroscopic observations were made on a few selected stars IRAS 17423−1755, IRAS 18237−0715, IRAS 19399+2312 and IRAS 22272+5435 (see Table 4 for their spectral types). Our results on several sources are compared with those taken earlier by Hrivnak, Kwok & Geballe (1994), Oudmaijer et al. (1995) and recently by Kelly & Hrivnak (2005). Here we report spectral variations in the CO first overtone bands in IRAS 22272+5435; and in H I lines in stars of early spectral type (hot PAGB stars). In both cases the time-scales of variability are short and may be associated with episodic mass-loss.

4.1 Variability of CO first overtone bands in IRAS 22272+5435

The spectra of this object of spectral type G5Ia show signatures that are probably indicative of its advanced stage of evolution in the PAGB phase. It was shown by Hrivnak et al. (1994) that the object shows episodes of mass-loss that was evident from month-scale

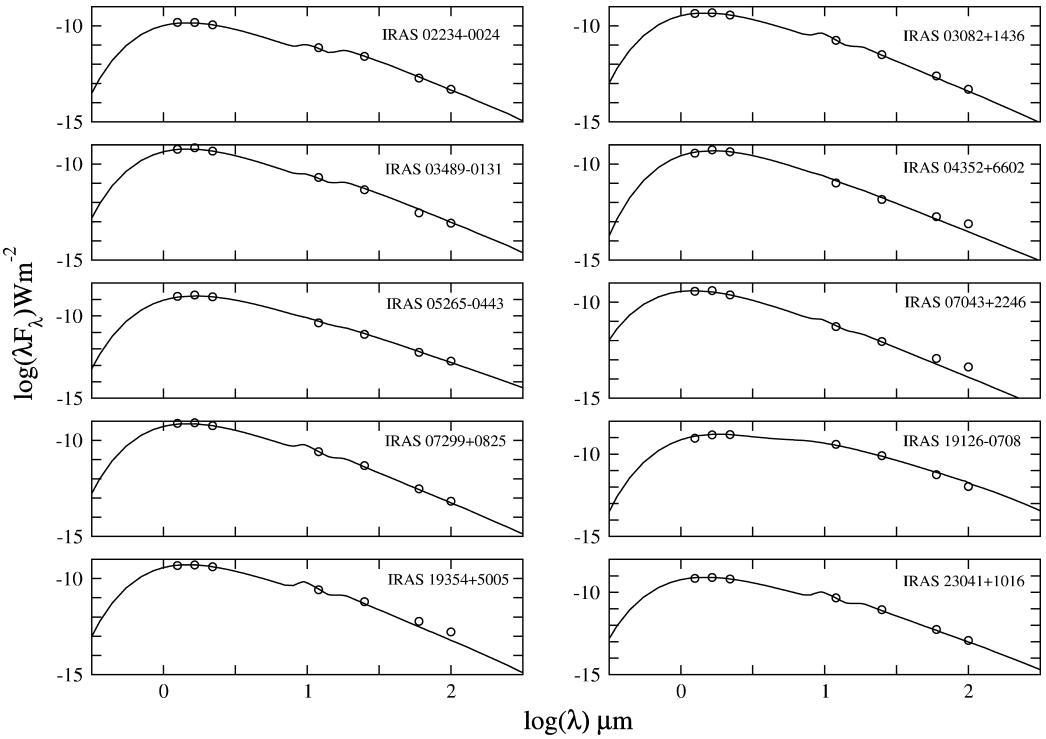

Figure 5. Model SEDs (full lines) of some M type stars compared with observed data from literature (open circles). See text for model parameters and explanation.

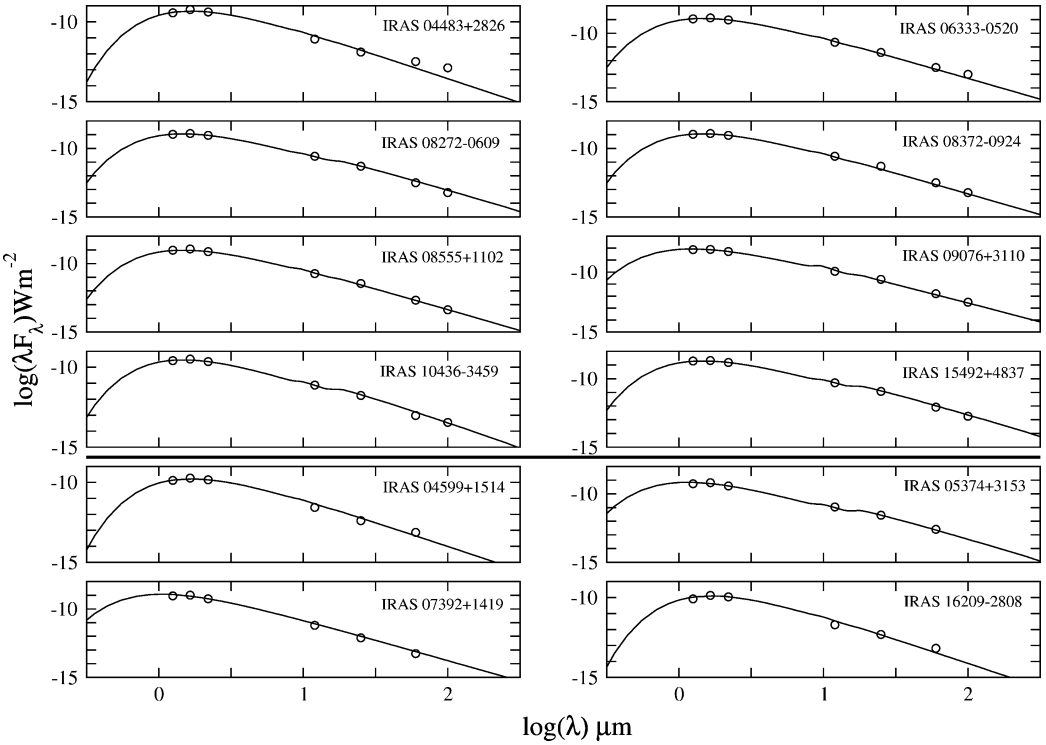

Figure 6. Model SEDs (full lines) of some SR type (in the top eight panels) and S type stars (in the bottom four panels below the horizontal line) compared with observed data from literature (open circles). See text for model parameters and explanation.

variability in its spectra. We obtained its spectra in *H* and *K* bands on two occasions separated by about 47 d (2006 November 4 and December 22). EWs for 2006 November 4 are given in Table 4. Fig. 8 shows the spectra and it is clear that the CO first overtone bands in the *K* band seen on November 4 were absent on December 22. But the Brackett H I absorption lines were seen in both *H*- and *K*-band spectra on both the observations. Interestingly the *H*-band second overtone bands of CO were *still present* in the spectra on

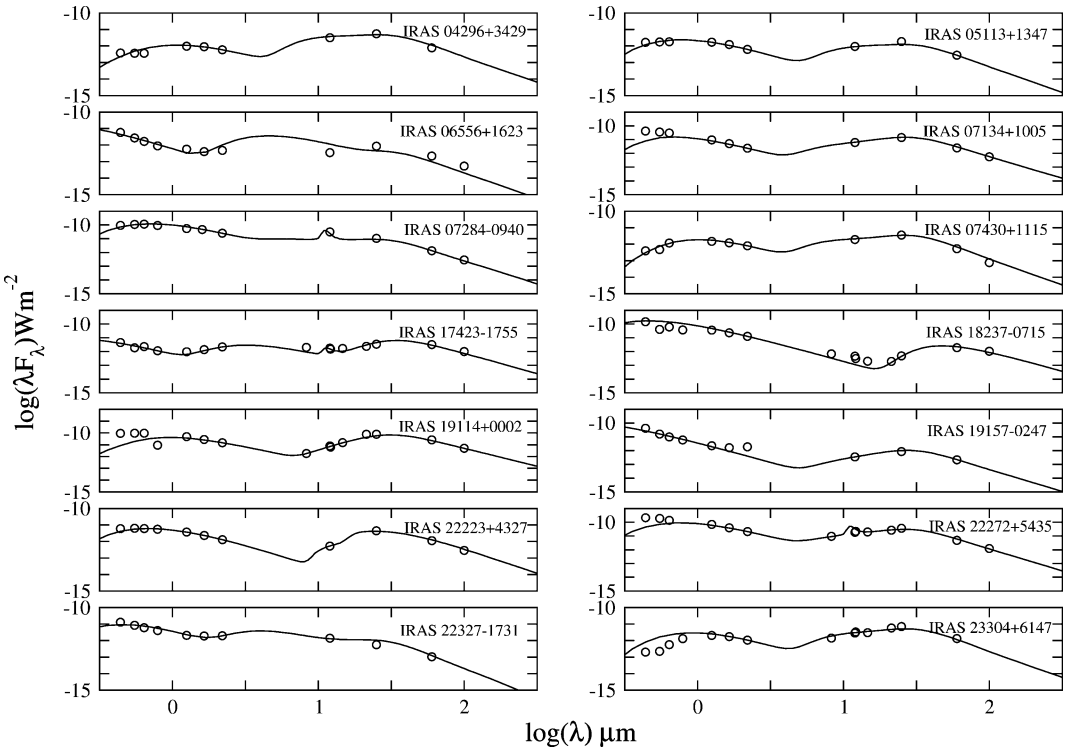

Figure 7. Model SEDs (full lines) of some PAGB stars compared with observed data from literature (open circles). See text for model parameters and explanation.

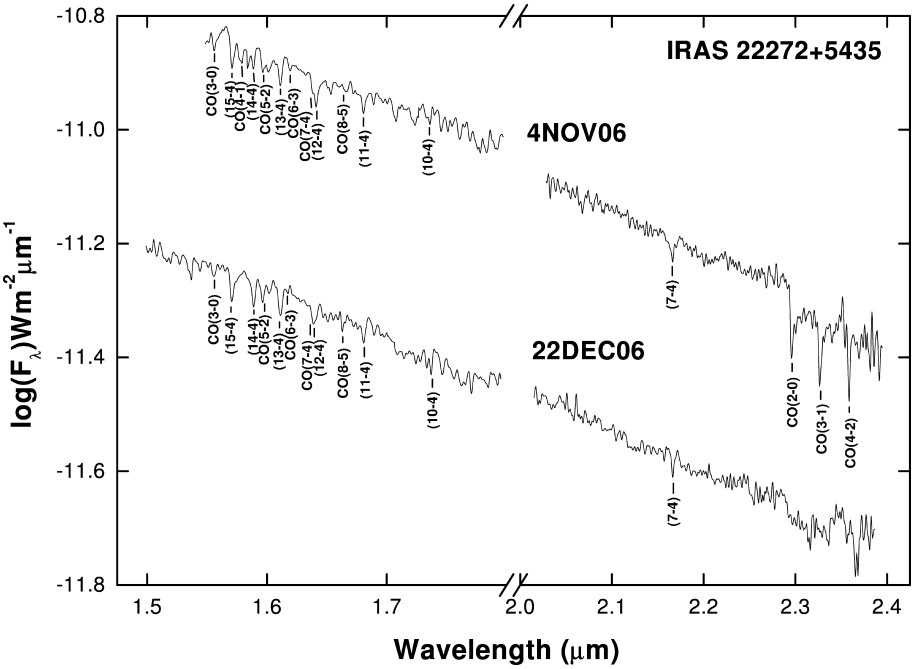

Figure 8. *H*- and *K*-band spectra of the PAGB star IRAS 22272+5435 taken on two dates from Mt Abu.

December 22. This shows that the mass-loss reached the outer regions of the atmosphere where the temperature is about a few hundreds of degree kelvin. The pulsations must be responsible for heating the matter in these regions resulting in the excitation of these lines and filling the absorption seen earlier.

We have found variability of spectra in a few other PAGB stars similar to IRAS 22272+5435. The *H*- and *K*-band spectra of IRAS 05113+1347, IRAS 19114+0002 and IRAS 22223+4327 were observed by Hrivnak et al. (1994). Our observations, made about 12 yr later, show clear indication of variability of CO in these stars which

might have occurred during the intervening period. In all these cases, the variations were found only in CO first overtone bands while the H I lines did not change. Oudmaijer et al. (1995) found CO second overtone bands in emission in the object IRAS 19114+0002 while our observations show near absence of these bands which can be attributed to mass-loss variations.

4.2 Variability of H I lines in IRAS 19399+2312

On the basis of the IRAS colours, Gauba et al. (2003) suggested that IRAS 19399+2312 (also known as V450 Vul) is a hot PAGB star possibly in transition to become a PPN. It was classified as a B1III star by Parthasarathy, Vijapurkar & Drilling (2000) but as B1IIIe by Kohoutek & Wehmeayer (1999). Recently, Greaves (2004) argued that being a possible member of the cluster NGC 6823, this star is unlikely to be a PAGB transition object but could be a spectroscopic type Be star. We made *JHK* band spectrometry at Mt Abu Observatory on this object on three occasions: first time on 2005 November 1 and then recently on 2007 May 15 and again on 2007 June 5–6 (the EWs obtained on 2007 June 6 are given in Table 4). The 2005 November 1 spectra showed some what shallow absorption in H I Paschen β and Brackett series lines. The later spectra however showed very prominent emissions in the H I lines, as well as a few permitted lines in He I and even forbidden lines in [Fe II] (1.60 μm) at relatively lower S/N (see Fig. 9). We also notice at a rather low S/N but still discernable CO ($\Delta v = 3$) lines in absorption. The appearance of the CO absorption lines is not usual in Be stars, as also the forbidden lines of metals ([Fe II]). In view of the appearance of forbidden lines (which was not reported earlier), and faint but significant CO lines, we believe that this object may as well be a transition object. To our knowledge, our observations are the first to show spectral variability in this object. From the ratios of the Brackett series lines which deviate from the Case B assumption (see e.g. Lynch et al. 2000), we infer variations in electron density or opacity in the atmosphere of this object associated with the H I line ratio variations that occurred between 2007 May 15 and 2007 June 5/6.

We made repeated observations on two more PAGB stars of early spectral type: for IRAS 17423−1755 (Be) on 2003 May 29 and 2007 May 13 and for IRAS 18237−0715 (Be) on 2004 May 28, 2006 Nov 3 and 2007 May 14. In Table 4, the EWs for IRAS 17423−1755 are for the date 2003 May 29; and for IRAS 18237−0715 the EWs are for 2006 November 3. We find variations in the intensities of H I Brackett series emission lines in both these objects. In the case of IRAS 18237−0715 the Brackett line ratios matched well with the Case B assumption on 2004 May 28 and 2006 November 3; while on 2007 May 14 the ratios deviated from Case B. Earlier in a detailed study Miroshnichenko et al. (2005) found spectral line variations in this object. This star did not show CO lines (Table 4). In the case of IRAS 17423−1755 on both the days of our observations the ratios deviated from Case B. These observations indicate the changes in electron density or opacity. This star showed CO first overtone lines in emission (Table 4). While Gauba et al. (2003) found emission lines in the optical spectra of IRAS 17423−1755 and 18237−0715 and hence termed these as transition objects, the nature of the latter object is ambiguous and could be a luminous blue variable according to the study of Miroshnichenko et al. (2005). Our IR spectra of this object closely resemble those of Miroshnichenko et al. (2005) and show P-Cygni type profiles with double peaks (see Fig. 1, top panel). Since we do not find CO lines in the spectra of this object it is likely that this object cannot possibly be a PAGB/transition object; or CO must have been dissociated.

In the case of the object IRAS 22327−1731 (type A0III) Oudmaijer et al. (1995) found that the CO bands as well as the H I lines were absent; our results (Table 4) show that the object displays the CO bands and H I Paschen β and Brackett γ in absorption, thus showing variability.

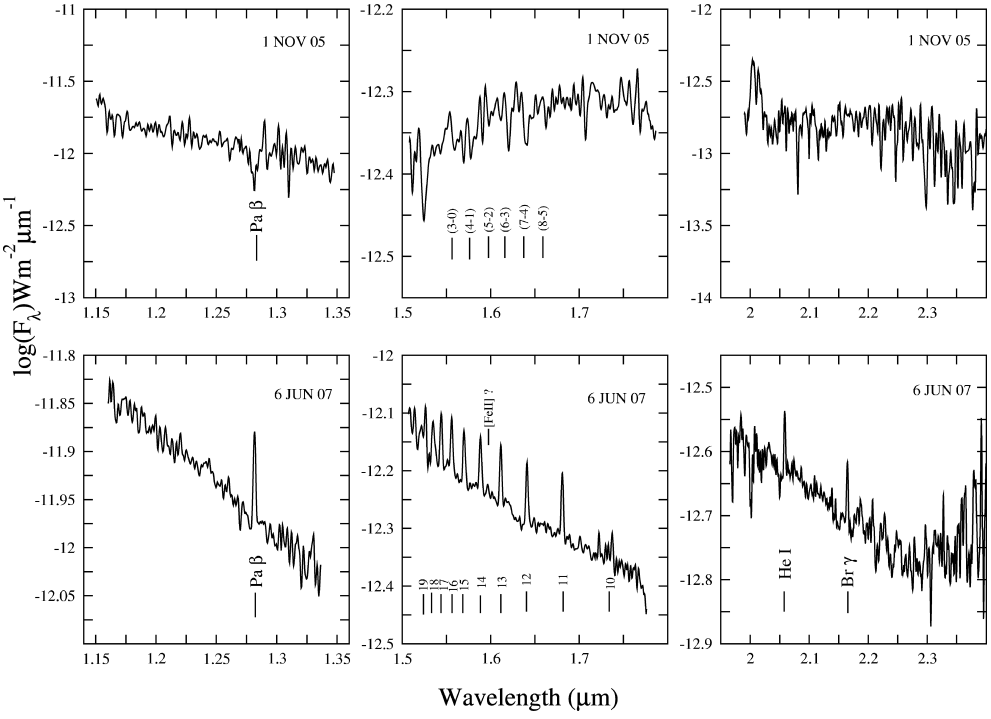

Figure 9. *J*-, *H*- and *K*-band spectra of the PAGB star IRAS 19399+2312 taken on two dates from Mt Abu.

© 2008 The Authors. Journal compilation © 2008 RAS, MNRAS **385,** 1076–1086

5 CONCLUSIONS

(i) The EWs of CO(3–0) show a trend of correlation with $[H-K]$ in M type; while in S stars the CO(3–0) shows a positive correlation with $[K-12]$.

(ii) The Mt Abu *H*- and *K*-band spectra also showed marked differences in the three types.

(iii) Archival *Spitzer* spectra of a few PAGB stars showing PAH emission features confirm their advanced stage of evolution into PPNe. There appears to be a dependence of the strength of the PAH features on the spectral type.

(iv) Modelling of SEDs of a number of the programme stars showed marked differences in various generic types. Model mass-loss rates for M and PAGB stars show an increasing trend with the colour $[K-12]$ in our sample stars.

(v) Our observations showed that several PAGB stars undergo short-term spectral variability that is indicative of ongoing episodic mass-loss. Cooler PAGB stars showed variation in CO first overtone lines. In contrast, the hot PAGB stars showed variation in H I lines. The hot PAGB star IRAS 19399+2312 is identified as a transition object.

ACKNOWLEDGMENTS

The authors sincerely thank the anonymous referee for critical comments that led to substantial improvement over the original version. This research was supported by the Department of Space, Government of India. We thank the Mt Abu Observatory staff for help in observations with NICMOS. We thank the *Spitzer* archival facilities. We acknowledge the DUSTY team for making available the code for the astronomy community. This research has made use of *IRAS*, 2MASS and *ISO* data bases.

REFERENCES

Bieging J. H., Rieke M. J., Rieke G. H., 2002, A&A, 384, 965
Bowen G. H., 1988, ApJ, 329, 299
Bujarrabal V., Castro-Carrizo A., Alcolea J., Sanchez Conteras C., 2001, A&A, 377, 868
Chen P. S., Gao H., Jorissen A., 1995, A&AS, 113, 51
Decin L., van Winckel H., Waelkens C., Bakkar E. J., 1998, A&A, 332, 928
Emerson D., 1996, Interpretation of Astronomical Spectra. Wiley, New York, p. 390
Feast M. W., 2000, in Wing R. F., ed., Proc. IAU Symp. 177, The Carbon Star Phenomenon. Kluwer, Dordrecht, p. 207
Fouquet P., Le Bertre T., Epchtein N., Guglielmo F., Kerschbaum F., 1992, A&AS, 93, 151
Gail H.-P., Sedlmayr E., 1987, A&A, 177, 186
Gail H.-P., Sedlmayr E., 1988, A&A, 206, 153
Garcia-Hernandez D. A., Manchado A., Garcia-Lario P., Dominguez-Tagle C., Conway G. M., Prada F., 2002, A&A, 387, 955
Garcia-Lario P., 2006, in Barlow M. J., Mendez R. H., eds, Proc. IAU Symp. 234, Planetray Nebulae in Our Galaxy and Beyond. Cambridge Univ. Press, Cambridge, p. 63
Gauba G., Parthasarathy M., Kumar B., Yadav R. K. S., Sagar R., 2003, A&A, 404, 305
Greaves J., 2004, IBVS, 5472, 1
Groenewegen M. A. T., de Jong T., 1998, A&A, 337, 797
Habing H., 1996, A&AR, 7, 97
Hinkle K. H., Hall D. N. B., Ridgway S. T., 1982, ApJ, 252, 697
Hony S., Van Kerckhoven C., Peeters E., Tielens A. G. G. M., Allamandola L. J., 2001, A&A, 370, 1030
Hoogzaad S. N., Molster F. J., Dominik C., Waters L. B. F. M., Barlow M. J., de Koter A., 2002, A&A, 389, 547
Hrivnak B. J., Bieging J. H., 2005, ApJ, 624, 331
Hrivnak B. J., Kwok S., 1999, ApJ, 513, 869
Hrivnak B. J., Kwok S., Geballe T. R., 1994, ApJ, 420, 783
Hrivnak B. J., Volk H., Kwok S., 2000, ApJ, 535, 275
Ivezic Z., Elitzur M., 1997, MNRAS, 287, 799
Jorissen A., Knapp G. R., 1998, A&AS, 129, 363
Kelly D. M., Hrivnak B. J., 2005, ApJ, 629, 1040
Kerschbaum F., Hron J., 1994, A&AS, 106, 397
Kleinmann S. G., Hall D. N. B., 1986, ApJS, 62, 501
Kholopov P. N. et al., 1988, General Catalogue of Variable Stars. Publishing House of the Academy of Sciences of the USSR, Moscow
Kohoutek L., Wehmeayer R., 1999, A&AS, 134, 255
Kwok S., 2000, The Origin and Evolution of Planetary Nebulae. Cambridge Univ. Press, Cambridge, p. 103, 151
Kwok S., 2004, Nat, 430, 985
Kwok S., Volk K., Hrivnak B. J., 1989, ApJ, 345, L51
Kwok S., Volk K., Hrivnak B. J., 1999, in Le Bertre T., Lebre A., Waelkens C., eds, ASP Conf. Ser. Vpl. 191, AGB Stars. Astron. Soc. Pac., San Francisco, p. 297
Lancon A., Rocca-Volmerange B., 1992, A&AS, 96, 593
Lancon A., Wood P. R., 2000, A&AS, 146, 217
Likkel L., Forveille T., Omont A., Morris M., 1991, A&A, 246, 153
Loidl R., Lancon A., Jorgensen U. G., 2001, A&A, 371, 1065
Loup C., Forveille T., Omont A., Paul J. F., 1993, A&AS, 99, 291
Lynch D. K., Rudy R. J., Mazuk S., Puetter R. C., 2000, ApJ, 541, 791
Miroshnichenko A. S. et al., 2005, MNRAS, 364, 335
Omont A., Loup C., Forveille T., te Lintel Hekkert P., Habing H., Sivagnanam P., 1993, A&A, 267, 515
Oudmaijer R. D., Waters L. B. F. M., van der Veen W. E. C. J., Geballe T. R., 1995, A&A, 299, 69
Parthasarathy M., Vijapurkar J., Drilling J. S., 2000, A&AS, 145, 269
Peeters E., Hony S., Van Kerckhoven C., Tielens A. G. G. M., Allamandola L. J., Hudgins D. M., Bauschlicher C. W., 2002, A&A, 390, 1089
Ramstedt S., Schoier F. L., Olofsson H., Lundgren A. A., 2006, A&A, 454, L103
Sahai R., Liechti S., 1995, A&A, 293, 198
Sloan G. C. et al., 2005, ApJ, 632, 956
Speck A. K., Hofmeister A. M., 2004, ApJ, 600, 986
Stasinska G., Szczerba R., Schmidt M., Siodmiak N., 2006, A&A, 450, 701
Tielens A. G. G. M., 2005, The Physics and Chemistry of the Interstellar Medium. Cambridge Univ. Press, Cambridge, p. 173
Ueta T., Meixner M., Moser D. E., Pyzovski L. A., Davis J. S., 2003, AJ, 125, 2227
van Winckel H., 2003, ARA&A, 41, 391
Vassiliadis E., Wood P. R., 1993, ApJ, 413, 641
von Helden G., Tielens A. G. G. M., van Heijnsbergen D., Duncan M. A., Hony S., Waters L. B. F. M., Meijer G., 2000, Sci, 288, 313
Volk K., Kwok S., Hrivnak B. J., 1999, ApJ, 516, L99
Wang H., Chen P. S., 2002, A&A, 387, 129
Whitelock P. A., Menzies J., Feast M. W., Marang F., Carter B., Roberts G., Catchpole R., Chapman J., 1994, MNRAS, 267, 711
Willson L. A., 2000, ARA&A, 38, 573
Winters J. M., Le Bertre T., Jeong K. S., Helling C., Sedlmayr E., 2000, A&A, 361, 641
Winters J. M., Le Bertre T., Jeong K. S., Nyman L.-A., Epchtein N., 2003, A&A, 409, 715
Woitke P., 2003, in Piskunov N. E., Weiss W. W., Gray D. F., eds, Proc. IAU Symp. Vol. 210, Modelling of Stellar Atmospheres. Astron. Soc. Pac., San Francisco, p. 387
Wood P. R., 1979, ApJ, 227, 220
Woodsworth A. W., Kwok S., Chen S. J., 1990, A&A, 228, 503

This paper has been typeset from a TEX/LATEX file prepared by the author.